arXiv:1610.08582v1 [quant-ph] 27 Oct 2016

Reviving the precision of multiple entangled probes in an open system by simple π-pulse sequences

Yang Dong, Xiang-Dong Chen, Guang-Can Guo, and Fang-Wen Sun*
Key Lab of Quantum Information, Chinese Academy of Sciences, School of physics, University of Science and Technology of China, Hefei, 230026, P.R. China, and Synergetic Innovation Center of Quantum Information & Quantum Physics, University of Science and Technology of China, Hefei, 230026, P.R. China
(Dated: October 28, 2016)

Quantum metrology with entangled states in realistic noisy environments always suffers from decoherence. Therefore, the measurement precision is greatly reduced. Here we applied the dynamical decoupling method to protect the N-qubit quantum metrology protocol and successfully revived the scaling of the measurement precision as N^{-k} with $k \in [5/6, 11/12]$. The degree of the precision revival, as determined by the noise spectrum distribution, indicates that the performance of the protected protocol can be further improved by controlling the noise spectrum. Such a protected protocol is proved to be universal for entanglement-based quantum metrology in the pure dephasing and relaxation noise, which should stimulate the development of practical quantum metrology for weak signal detection of microscopic physics.

PACS numbers: 42.50.Lc, 03.65.Yz, 06.20.-f

I. INTRODUCTION

Improving the resolution of spectroscopy is the heart of metrology. It is also of importance for science and technology. Over the past few decades, improvements with quantum resources [1–6] have been widely explored. Among these, the entanglement-based spectroscopy [7–9] is an impressive method. It has been shown that N-particle maximally entangled states in fully coherent evolution (FCE) can be used to achieve the Heisenberg quantum limit (HQL), in which the uncertainty can in principle scale as N^{-1}. However, the maximally entangled states are fragile in realistic noisy environments and the notorious quantum decoherence would reduce the precision to the standard quantum limit (SQL) scaling of $N^{-1/2}$ [10] in the detection process. To keep the entanglement-based method alive, it is necessary to avoid or fight against the decoherence. Recent studies have shown that a super-classical scaling relationship can survive [11] by avoiding the spatial direction of Markovian noise. Generally, it is difficult to address Markovian noise and draw the coherence from the environment [10]. However, in solid spin systems [12–15], the Markovian approximation treatment of the environment is not always valid [16]. Recently, the $N^{-3/4}$ scaling of uncertainty of detection a physical parameter has been demonstrated in the non-Markovian dephasing environments [16–18]. Therefore, the optimal measurement precision with maximally entangled states can be improved by beating the non-Markovian noise of the sensor system, thus providing an effective method to revive the HQL in realistic noisy environments.

In the past few decades, the dynamical decoupling (DD) method has been shown to be highly effective for suppressing decoherence by filtering of the noise spectrum [19–26]. It has been well applied in one-qubit and two-qubit quantum information processes [27, 28]. Here we combine the traditional quantum metrology strategies, the quantum-classical (QC) and quantum-quantum (QQ) metrology protocol [4, 5], with the DD method to construct protected QC (P-QC) and protected QQ (P-QQ) protocols as shown in Fig. 1. The new protected protocols are robust against pure dephasing and longitudinal relaxation noise and can be used to revive the measurement precision scaling of N^{-k} with $k \in [5/6, 11/12]$. It is much better than the presented in Refs. [16–18]. The index k, which evaluates the degree of revival of the measurement precision by the DD protection method, is determined by the shape of the noise spectrum, especially its high frequency component. Consequently, in addition to extending the system coherence time, the performance of quantum metrology can be highly improved by changing the shape of the system noise spectrum. Furthermore, by studying a general quantum metrology protocol, the DD protection method is proved to be universal for re-

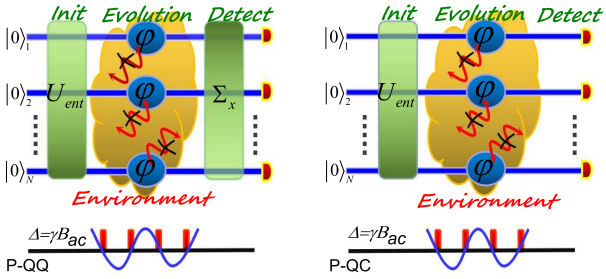

FIG. 1. Two protected quantum metrology protocols with N sensor qubits. The CPMG sequences (red rectangles) are applied on each sensor qubit during the detection of a weak AC magnetic field to protect sensor qubits.

* fwsun@ustc.edu.cn

viving the advantage of the entanglement-based quantum metrology in pure dephasing and longitudinal relaxation noisy environments. A hybrid system composed of a superconducting circuit and N NV^- centers in bulk diamond can be applied to present the protected quantum metrology protocol with current techniques. Therefore, the P-QQ and P-QC metrology protocols will stimulate the development of practical quantum metrology application in realistic environments and open a new avenue for weak signal detection.

II. INDEPENDENT PURE DEPHASING NOISE MODEL

Here we consider a quantum metrology protocol in a practical decoherent environment that can be described with a fully quantum independent spin-boson noise model [16, 20, 21, 24, 29]. The sensor system consists of N two-level qubits, where $|0_j\rangle$ ($|1_j\rangle$) denotes the ground (excited) state of the jth qubit with the eigenvalue of -1 (1). The interaction on the sensor qubits is given by

$$\begin{aligned} H =& \sum\nolimits_{j=1}^{N} \frac{\sigma_{z,j}}{2} \sum\nolimits_{i} \lambda_{i,j}(b_{i,j}^{\dagger} + b_{i,j}) \\ &+ \sum\nolimits_{j=1}^{N} \sum\nolimits_{i} \omega_{i,j} b_{i,j}^{\dagger} b_{i,j}, \end{aligned} \tag{1}$$

where $\lambda_{i,j}$ denotes the coupling strength between the jth sensor qubit and the environment. $\sigma_{x,j}, \sigma_{y,j}, \sigma_{z,j}$ are the jth sensor qubit Pauli matrices. Here, the environment is regarded as a bosonic bath with the annihilation (creation) operator $b_{i,j}$ ($b_{i,j}^{\dagger}$) and frequency $\omega_{i,j}$ interacting with the jth sensor qubit. The relevant spin-boson bath property of the jth sensor qubit is controlled by the completely high-energy cutoff noise model [29]:

$$\begin{aligned} J_j(\omega) &= \sum\nolimits_{i} |\lambda_{i,j}|^2 \delta(\omega - \omega_{i,j}) \\ &= 2\alpha_j \omega \Theta(\omega_{D,j} - \omega), \end{aligned} \tag{2}$$

where α_j is the dimensionless coupling strength and $\omega_{D,j}$ is the cutoff frequency. Without loss of generality, we discuss the quantum metrology for the detection of an AC magnetic field B. The sensor state will gain the shift of $\Delta = \gamma B$ after the interaction with the magnetic field, where γ is the gyromagnetic ratio of the sensor spin. Therefore, when the sensor system is in this field, the evolution process can be described by

$$H_s = \Delta \cos \omega t \sum\nolimits_{j=1}^{N} \sigma_{z,j} + H. \tag{3}$$

III. THE PROTECTED QUANTUM METROLOGY PROTOCOL

Because the final measurement is the only difference between the P-QC and P-QQ metrology protocols, we first discuss the P-QQ metrology protocol. The protected quantum metrology protocol can be divided into three typical steps [4, 5]:

i) Initialization of the sensor system. Generally, quantum metrology can be well realized with the Greenberger-Horns-Zeilinger ($|GHZ\rangle$) state described by

$$|GHZ\rangle = D_y(\pi/2)\,|G\rangle = [|G\rangle + |E\rangle]/\sqrt{2}, \tag{4}$$

where $D_y(\pi/2) = \exp(-i\pi\Sigma_y/4)$ and $\Sigma_y = -i\,|E\rangle\langle G| + i\,|G\rangle\langle E|$ with $|G\rangle = \Pi_{j=1}^{N}|0_j\rangle$ ($|E\rangle = \Pi_{j=1}^{N}|1_j\rangle$).

ii) Evolution in the physical field to be detected. The sensor state will gain a relative phase shift after interaction with the field for time τ. In the protected measurement process, the evolution is accompanied by symmetric timing dynamical decoupling Carr-Purcell-Meiboom-Gill (CPMG) sequences [30], which can be described by the operation $\Pi_{x,N} = \Pi_{j=1}^{N} i\sigma_{x,j}$ acting on the sensor system for n times, as shown in Fig. 1. When the AC field picks up a negative sign at $\delta_m = \frac{m-1/2}{n}\tau$ with $m = 1, ...n$, the π pulse appears and flips all the sensor qubits to generate an additive phase and dynamically decouple from fluctuating noisy bath. Therefore, the evolution process can be represented as

$$|\Psi\rangle = R\,|GHZ\rangle\,, \tag{5}$$

where

$$\begin{aligned} R =& \mathrm{e}^{-iH_s(\delta_{n+1}-\delta_n)}\Pi_{x,N}\mathrm{e}^{-iH_s(\delta_n-\delta_{n-1})}\Pi_{x,N}\cdots \\ &\cdots \mathrm{e}^{-iH_s(\delta_2-\delta_1)}\Pi_{x,N}\mathrm{e}^{-iH_s(\delta_1-\delta_0)}. \end{aligned} \tag{6}$$

iii) Detection process. After the detection with $\Sigma_x = |E\rangle\langle G| + |G\rangle\langle E|$, the signal will be

$$s_n(\tau) = \langle G|D_y^{\dagger}(\pi/2)R^{\dagger}\Sigma_x R D_y(\pi/2)\,|G\rangle\,. \tag{7}$$

The shift Δ can be estimated by repeating the above measurement processes $l = T_t/\tau$ times. Here, T_t is the total duration and τ is the interrogation time of the experiment. The final signal can be directly calculated:

$$s_n(\tau) = \cos N\varphi \exp\left(-2\chi_n\right), \tag{8}$$

where

$$\varphi = \frac{4\Delta\tau}{\pi},$$

$$\chi_n = \sum\nolimits_{j=1}^{N} \int_0^{+\infty} \frac{F_n(\omega\tau)J_j(\omega)}{4\omega^2} \coth(\omega/2k_BT)\mathrm{d}\omega,$$

$$F_n(\omega\tau) = 8\sin^4\frac{\omega\tau}{4n}\sin^2\frac{\omega\tau}{2}/\cos^2\frac{\omega\tau}{2n}.$$

Here k_B is the Boltzmann constant and T is the temperature of the environment. The behavior of χ_n, which is the result of the independent noise model for the

most realistic solid system, governs the detection precision. The phase is linearly related to the number of sensor qubits N and interrogation time τ. Simply, $n = 1$ corresponds to the spin echo sequence with $\chi_1 = \sum_{j=1}^{N} \int_0^{+\infty} \frac{F_1(\omega\tau)J_j(\omega)}{4\omega^2} \mathrm{d}\omega$ and $F_1(\omega\tau) = 8\sin^4\frac{\omega\tau}{4}$. When the measurement operator Σ_x is replaced with $(-i)^N \Pi_{x,N}/2$, the P-QQ metrology protocol is transferred to the P-QC metrology protocol as shown in Fig. 1. In this case, the above conclusions are also valid.

IV. RESULTS OF THE PROTECTED QUANTUM METROLOGY PROTOCOL WITH CPMG SEQUENCES

For $T \to 0K$, corresponding to the low-temperature limit, $\chi_n = \sum_{j=1}^{N} \int_0^{+\infty} \frac{F_n(\omega\tau)J_j(\omega)}{4\omega^2} \mathrm{d}\omega = N \int_0^{+\infty} \frac{F_n(\omega\tau)\bar{J}(\omega)}{4\omega^2} \mathrm{d}\omega$, where $\bar{J}(\omega)$ is the equivalent noise spectral function. When $\omega_D\tau << 1$, the decoherence process can be characterized by

$$\chi_n \approx \alpha N \tau^6 \tag{9}$$

with $\alpha = \int_0^{+\infty} \frac{\omega^4 \bar{J}(\omega)}{2\cdot(4n)^4} d\omega$. The precision enhancement over SQL with entangled probe [16] is $r = N^{(v-1)/2v}$ where v is the power law index of τ. Therefore, for the present protected protocol with the $|GHZ\rangle$ state, the enhancement is $r = N^{5/12}$ and the final precision is $\delta\Delta_n \sim N^{-11/12}$, very close to the HQL as shown in Fig. 2. Even for the simplest spin-echo sequence, the optimal precision of entangled probes follows the characteristic scale as $N^{-7/8}$, which is superior to $N^{-3/4}$ scaling obtained for the non-Markovian noise without DD protection [16–18]. The optimal interrogation time of protected protocol is reasonable: $\tau \approx 0.1/(12\alpha N)^{1/6}$ or AC signals with frequencies of approximately 10kHz $\sim$ 100kHz after considering the solid spin sensor system [18, 31, 32].

V. HIGH-TEMPERATURE LIMIT AND THE LONGITUDINAL SPIN RELAXATION

However, the high-energy cutoff noise model is too simple to describe the entire physical noise behaviors and the condition $T \to 0$K is always difficult to be achieved for a realistic sensor system, especially in the solid spin systems surrounded by magnetic nuclei. When $T \to$ mK, the high-temperature approximation ($k_B T >> \gamma_n B$) is always valid for typical experimental conditions [33] with $\gamma_n \sim$ kHz/G and $B \sim$ 100G, where γ_n is the gyromagnetic ratio of the proton. Therefore, in these realistic systems, the decoherence of the sensor system is governed by thermal fluctuations and the system exhibits classical behavior [21]. The effect of the environment can be described by the classical Hamiltonian

$$H = \sum_{j=1}^{N} f_j(t)\sigma_{z,j}/2, \tag{10}$$

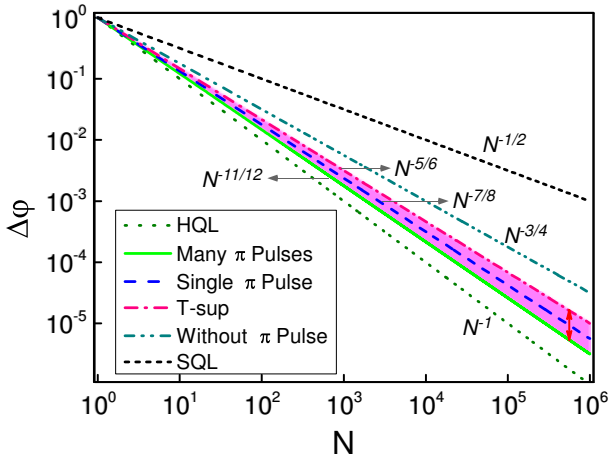

FIG. 2. Scaling of the measurement uncertainty versus the number of sensor qubits. The SQL and HQL scalings are shown with black short-dashed and olive dotted lines, respectively. The dark cyan dashed dot-dotted, blue dashed and green solid lines represent the scalings of $\delta\Delta$ with no pulse, a single π pulse and many π pulses, respectively, at low-temperature with a high-energy cutoff noise model. The region marked by the rad arrow indicates the scales $\delta\Delta$ after taking temperature into consideration for many π pulses under non-Markovian dephasing.

where $f_j(t)$ is a classical random noise field distribution on the jth sensor qubit with $\langle f_j(t)\rangle = 0$ and $\langle f_j(t_1)f_j(t_2)\rangle = g_j(t_1 - t_2)$. After application of the protected metrology protocol, we can obtain a similar result

$$\lim_{T\to+\infty} s_n(\tau) = \cos N\varphi \exp\left(-2 \lim_{T\to+\infty} \chi_n\right) \tag{11}$$

with

$$\lim_{T\to+\infty} \chi_n = \sum_{j=1}^{N} \int_0^{+\infty} \frac{F_n(\omega\tau)p_j(\omega)}{\pi\omega^2} \mathrm{d}\omega, \tag{12}$$

where $4p_j(\omega)/\pi$ is the classical noise power spectrum corresponding to the Fourier transform of $g_j(t)$. Here we consider two spin bath models with Lorentzian and Gaussian noise spectral density, respectively. The results are presented in Table 1.

TABLE I. Results for two common classical noise models with $\tau < \tau_c$. The subscript is the number of π pulses applied on each sensor qubit.

	χ_0	$\delta\Delta_0$	χ_1	$\delta\Delta_1$	χ_2	$\delta\Delta_2$
Lorentzian	$N\tau^2$	$N^{-3/4}$	$N\tau^3$	$N^{-5/6}$	$N\tau^3$	$N^{-5/6}$
Gaussian	$N\tau^2$	$N^{-3/4}$	$N\tau^4$	$N^{-7/8}$	$N\tau^6$	$N^{-11/12}$

When the correlation time τ_c of the noisy environment is longer than the interrogation time τ, the present protection protocol can also beat the SQL again in the common realistic experimental environment as shown in the Table 1. Additionally, the degree of reviving of the

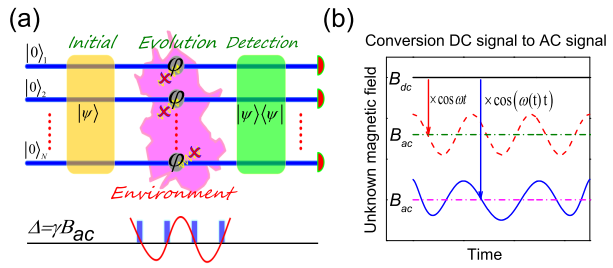

FIG. 3. (a) General protected quantum metrology protocol. Initial sensor system in $|\psi\rangle$ state is placed into the magnetic field for time τ accompanied by DD sequences. The measurement operation is $|\psi\rangle\langle\psi|$. (b) The DC field is converted to arbitrary AC field by rotating the sensor system to match the DD sequences for the protected quantum metrology protocol well.

measurement precision by the DD sequences is determined by the shape of the noise spectrum, especially its high frequency component. The filter function of DD sequences exhibits weaker performance in the high-frequency region. Therefore, the measurement precision under the Gaussian noise spectrum is better than under the Lorentzian noise spectrum because of the much smaller high-frequency component of the Gaussian noise spectrum. This indicates that, in addition to the decoherence time, the quantum metrology performance is also controlled by the shape of the system noise spectrum. Moreover, Uhrig-DD(UDD) was proved to be universal for the suppression of qubit longitudinal spin relaxation noise [24]. Because the CPMG sequence and UDD sequence have an intersection: the spin echo sequence and two π pulses sequence, using a similar derivation, it can be shown that our protected protocols are also valid for the longitudinal relaxation noise. However, $p_j(\omega)$, which changes with different sensor qubits and local magnetic field, is always too complicated to be described by a specific function in reality [15, 34, 35]. Recent experiment showed that $\chi_n \approx \alpha\tau^v$ with $v \in (3, 6)$ for single qubit under DD sequence [36]. Hence, it indicates the optimal resolution of entangled probe follow a characteristic scaling as N^{-k} with $k \in [5/6, 11/12]$ in high temperature, as shown in Fig. 2 with pink area. This result is also better than the previously obtained results [16–18], demonstrating the advantages of the protected protocols.

VI. GENERALIZATION OF PROTECTED QUANTUM METROLOGY PROTOCOL

The above conclusion is drawn based on the detection of an AC physical field with a specific initial state—$|GHZ\rangle$. Such a protected quantum metrology protocol can also be generalized for wider practical applications [4, 5, 10].

i) Generalization of the sensor state. As shown in Fig. 3(a), we consider a general quantum metrology protocol with an initial state $|\psi\rangle$ and detection operator $|\psi\rangle\langle\psi|$ that can be used to achieve the HQL in FCE. Therefore, the evolution generator [4] $h_{s,c} = \sum_{j=0}^{N} \sigma_{z,j}$ should satisfy the relationship $\delta h_{s,c} \propto N$ to obtain the measurement precision scaling as $1/N$

$$\begin{aligned}\min\{\delta\Delta_{c,n}\} &\leqslant \delta\Delta_{c,n}|_{\varphi\to 2m\pi} \\ &\approx \sqrt{\frac{\pi^2}{16\tau^2 l\delta h_{s,c}^2}} \propto 1/N,\end{aligned} \tag{13}$$

where m is an integer. After considering the completely high-energy cutoff noise model, the result with the CPMG protection sequences is

$$\begin{aligned}min\{\delta\Delta_n\} &\leqslant \delta\Delta_n|_{\substack{N\varphi=2m\pi+\theta,\theta\approx 0.01 \\ \tau\approx 0.1/(\alpha N)^{1/6}}} \\ &\approx \sqrt{\frac{\theta^2\delta h_{s,c}^2/4 + 2\alpha N\tau^6}{l\theta^2|d\varphi/d\Delta|^2\delta h_{s,c}^4/4}}\Bigg|_{\substack{\theta\approx 0.01 \\ \tau\approx 0.1/(\alpha N)^{1/6}}} \\ &\propto N^{-11/12}.\end{aligned} \tag{14}$$

This shows that the general protected quantum metrology protocol is universal, thus preserving the advantage of an arbitrary entangled state that can be used to beat the SQL in pure dephasing noisy environment. And it is also valid for longitudinal relaxation noise. There exist some other entangled states that possess the character of super-classical scaling relationship in the FCE beyond the above quantum metrology protocol and are relatively easy to generate [18]. So in these cases, the protection with the DD method is always valid because it changes the decoherence process when $\tau \approx 0.1/(\alpha N)^{1/6}$. For example, a spin cat state or a two-axis twisted state can obtain $\delta\Delta_n \propto N^{-k}$ with $k \in [5/6, 11/12]$.

ii) Generalization of detection frequency region. In the above discussion, an AC field can be detected well with the protected protocol. For the measurement of a DC field, a simple method is to rotate the sensor system in the field and introduce an AC interaction. Hence, the DC physical field can be intentionally transferred to an arbitrary AC field on purpose, as shown in Fig. 3(b). For example, with the advances in laser-induced rotation technology, the rotation speed of the solid sensor system, such as a negatively charged nitrogen-vacancy center in diamond [37], can be controlled with a circularly polarized trapping laser beam [38, 39]. Such a rotation can be modified to extend the detection frequency to the MHz [39]. Moreover, the controlled frequency may be fitted to the UDD sequence [20, 21] to optimally protect the sensor state in noisy environments, further enhancing the estimation resolution approaching the HQL.

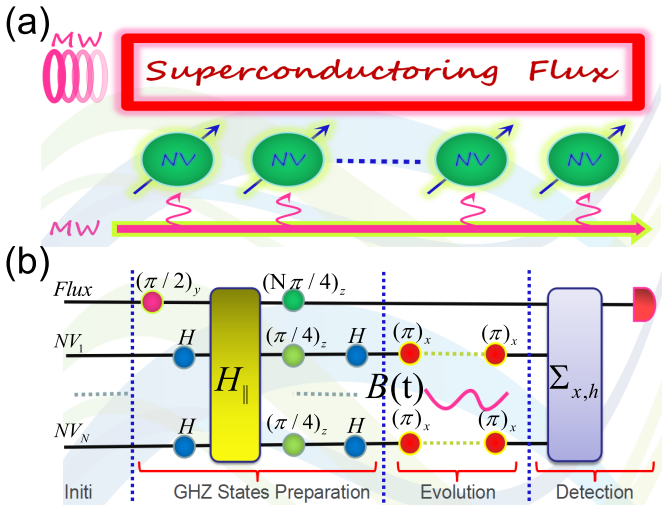

FIG. 4. (a) The schematic diagram of hybrid sensor system. All qubits can be operated by microwave pulse. (b) The quantum circuit for creating the $N+1$-qubits GHZ state and detecting weak AC physical field. Here, $(\theta)_b = e^{-i\theta\hat{\sigma}_b/2}$ and $b = x, y, z$.

VII. CONSTRUCTION OF PROTECTED METROLOGY PROTOCOL WITH HYBRID SYSTEM

As shown in Fig. 4(a), a hybrid system composed of a superconducting circuit and N NV^- centers in bulk diamond can be used to present the protected quantum metrology protocol, where the superconducting flux qubit is a control and readout qubit and spin states in NV center are memory and sensor qubits. In the interaction picture, the Hamiltonian of the hybrid sensor system can be written as [18]:

$$H_{total} = H_{||} + H_{\perp}, \tag{15}$$

with

$$H_{||} = \hbar g_1 \hat{\sigma}_z^{(c)} \hat{J}_z^{(m)}, \tag{16}$$

$$H_{\perp} = \hbar g_2 (\hat{\sigma}_+^{(c)} \hat{J}_-^{(m)} + \hat{\sigma}_-^{(c)} \hat{J}_+^{(m)}), \tag{17}$$

where $H_{||}(H_{\perp})$ is the longitudinal (transverse) interaction between control qubit and sensor qubit, $\hat{\sigma}_z^{(c)}$ denotes Pauli operator acting on control qubit, $\hat{J}_z^{(m)}$ is collective spin operator on sensor qubit, $\hat{\sigma}_{\pm}^{(c)}(\hat{J}_{\pm}^{(m)})$ is a ladder operator on control (sensor) qubit. In order to briefly demonstrate the original idea to show the P-QQ metrology protocol, we make use of longitudinal Hamiltonian [10] to create $(N+1)$-qubit $|GHZ+\rangle = [|G\rangle_h + |E\rangle_h]/\sqrt{2}$,where $|G\rangle_h = |0\rangle_f \prod_{j=1}^{N} |0\rangle_{NV_j^-}$ and $|E\rangle_h = |1\rangle_f \prod_{j=1}^{N} |1\rangle_{NV_j^-}$. The single-qubit logic gate can be made with microwave operation and the two-qubit Controlled-NOT gate, or CNOT, can be directly constructed with

$$U_{CNOT} = (I \otimes H)\, U_{CZ}\, (I \otimes H), \tag{18}$$

and

$$U_{CZ} = \sqrt{i} e^{-i\frac{\pi}{4}\sigma_z^c} e^{-i\frac{\pi}{4}\sigma_z^t} e^{-i\frac{3\pi}{4}\sigma_z^c\sigma_z^t}, \tag{19}$$

where I, H and U_{CZ} are identity, Hadamard, and Controlled-Z gates, respectively. σ_z^c (σ_z^t) denotes pauli operator acting on the control (target) qubit. Hence, the $(N+1)$-qubit CNOT gate can be created:

$$\prod_{j=1}^{N} C_f NOT_{NV_j^-} = \prod_{j=1}^{N} H_j \prod_{j=1}^{N} U_{CZ,j} \prod_{j=1}^{N} H_j, \tag{20}$$

$$\prod_{j=1}^{N} U_{CZ,j} = \prod_{j=1}^{N} \sqrt{i^N} e^{-i\frac{N\pi}{4}\hat{\sigma}_z^{(c)}} e^{-i\frac{\pi}{4}\hat{J}_z^N} e^{-i\frac{3\pi}{4g_1}H_{||}}, \tag{21}$$

where $C_f NOT_{NV_j^-}$ denotes a CNOT gate which flux is control qubit and NV_j^- is target qubit, H_j is a Hadamard gate acting on NV_j^-, and $U_{CZ,j}$ is Controlled-Z gate acting on flux and NV_j^-. Omitting the global phase $\sqrt{i^N}$, we can get $(N+1)$-qubit $|GHZ+\rangle$ state and those processes can be denoted by an operations $U_{ent,h}$. If DD sequences [27, 28] are interleaved in the generation processes, the decoherence effects can be neglected. It also holds for detection process. Then the hybrid system evolves in the weak AC physical field for time τ with symmetric timing dynamical decoupling CPMG sequence on each sensor qubit. Finally, the measurement operation can be constructed in this way:

$$\begin{aligned}\Sigma_{x,h} &= |G\rangle_{hh}\langle E| + |E\rangle_{hh}\langle G| \\ &= \frac{|GHZ+\rangle\langle GHZ+|}{2} - \frac{|GHZ-\rangle\langle GHZ-|}{2},\end{aligned} \tag{22}$$

with $|GHZ-\rangle = [|G\rangle - |E\rangle]/\sqrt{2}$. The former measurement operator is created by $|GHZ+\rangle\langle GHZ+| = U_{ent,h}|G\rangle_{hh}\langle G|U_{ent,h}^{-1}$. By just adding a $(\pi)_z$ gate on flux qubit following closely after $U_{ent,h}$, the measurement operator of $|GHZ-\rangle\langle GHZ-|$ is created and the measurement operation Σ_x can be obtained. So briefly, the P-QQ metrology protocol can be put into practice with current system and technology with simple few manipulations. It also holds for P-QC and the general protected quantum metrology protocol.

VIII. CONCLUSION

By fighting the pure dephasing and longitudinal relaxation noisy environment with the DD method on an N-qubit quantum metrology protocol, we successfully revive the measurement precision of the $|GHZ\rangle$ state scaling as $N^{-11/12}$ at low temperatures. Even in the high-temperature region, the precision can still be improved

to N^{-k} with $k \in [5/6, 11/12]$. The degree of revival of the measurement precision with the DD protection is primarily determined by the high frequency component of the noise spectrum, indicating that the performance of quantum metrology in realistic environments is highly dependent on the details of the noise spectrum in addition to the coherence time. Moreover, we generalize our protocol and prove that it can maintain the validity of the entanglement-based method in pure dephasing and longitudinal relaxation noisy environments. For experimental realization, the use of hybrid quantum circuits based on superconducting circuits interacting with quantum solid systems is very promising with current quantum techniques. Therefore, such a protected quantum metrology would show its high practical potential for the detection of ultra-weak physical parameters in realistic noisy environments.

ACKNOWLEDGMENT

We thank Hailin Wang for fruitful discussions. This work was supported by the Strategic Priority Program(B) of the Chinese Academy of Sciences (No. XDB01030200), the National Natural Science Foundation of China (Nos. 11374290, 61522508, 91536219, 11504363), the Fundamental Research Funds for the Central Universities and the China Postdoctoral Science Foundation (No.2015M571935).

Appendix A: The calculation of signal expression

The signal $s_n(\tau) = \langle G|D_y^\dagger(\pi/2)R^\dagger\Sigma_x R D_y(\pi/2)\,|G\rangle$ can be calculated with the unitary transformation

$$U = \exp\left(\sum\nolimits_{j=1}^{N} \sigma_{z,j}K_j\right), \tag{A1}$$

with $K_j = \sum_{i=1} \frac{\lambda_{i,j}}{2\omega_{i,j}}(b_{i,j}^\dagger - b_{i,j})$. Under this transformation, H_s can be diagonal

$$H_s^{ef} = H^{ef} + \Delta\cos\omega t\sum\nolimits_{j=1}^{N}\sigma_{z,j}, \tag{A2}$$

with $H^{ef} = \sum_{j=1}^{N}\sum_i \omega_{i,j}b_{i,j}^\dagger b_{i,j} + E - \sum_{j=1}^{N}\int_0^{+\infty}\frac{J_j(\omega)}{\omega}d\omega$. Here, E denotes the energy offset of sensor system. Therefore, arbitrary quantum operator F has a new form: $F^{ef} = UFU^\dagger$. So the signal can be expressed as

$$s_n(\tau) = \langle G|D_y^{ef\dagger}(\pi/2)R^{ef\dagger}\Sigma_x^{ef}R^{ef}D_y^{ef}(\pi/2)\,|G\rangle\,. \tag{A3}$$

Since H_s and even number π-pluses do not cause spin flip, we can directly get

$$\begin{aligned} s_n(\tau) &= -\frac{i}{2}\langle G|\Sigma_y^{ef}R^{ef\dagger}\Sigma_x^{ef}R^{ef}\,|G\rangle \\ &\quad + \frac{i}{2}\langle G|R^{ef\dagger}\Sigma_x^{ef}R^{ef}\Sigma_y^{ef}\,|G\rangle \\ &= \mathrm{Im}\langle G|\Sigma_y^{ef}R^{ef\dagger}\Sigma_x^{ef}R^{ef}\,|G\rangle\,, \end{aligned} \tag{A4}$$

with $\langle G|\Sigma_x^{ef}\,|G\rangle = \langle E|\Sigma_x^{ef}\,|E\rangle = \langle G|\Sigma_y^{ef}\,|G\rangle = \langle E|\Sigma_y^{ef}\,|E\rangle = 0$.

By defining the time-dependent operators

$$F^{ef}(\tau) = \exp(iH^{ef}\tau)F^{ef}\exp(-iH^{ef}\tau), \tag{A5}$$

the signal can be expressed as

$$s_n(\tau) = \mathrm{Im}\left[e^{-i\varphi_n}\langle G|\Sigma_y^{ef}(0)\tilde{R}^\dagger\Sigma_x^{ef}(\tau)\tilde{R}\,|G\rangle\right] \tag{A6}$$

with

$$\begin{aligned} \varphi_n &= \sum\nolimits_{i=0}^{n}\int_{\delta_i}^{\delta_{i+1}}\Delta\cos\omega t dt \\ &= \frac{4\Delta N\tau}{\pi}, \end{aligned} \tag{A7}$$

$$\tilde{R} = \Pi_{x,N}^{ef}(\delta_n)\Pi_{x,N}^{ef}(\delta_{n-1})\cdots\Pi_{x,N}^{ef}(\delta_1). \tag{A8}$$

Similar relations [21] are also held

$$\Pi_{x,N}^{ef}(\delta_i)\,|G/E\rangle = i^N\exp\left(\pm 2\sum\nolimits_{j=1}^{N}K_j(\delta_i)\right)|E/G\rangle\,, \tag{A9}$$

$$\Sigma_x^{ef}(\tau)\,|G/E\rangle = \exp\left(\pm 2\sum\nolimits_{j=1}^{N}K_j(\tau)\right)|E/G\rangle, \tag{A10}$$

$$\Sigma_y^{\mathrm{ef}}(\tau)\,|G/E\rangle = \mp i\exp\left(\pm 2\sum\nolimits_{j=1}^{N}K_j(\tau)\right)|E/G\rangle\,. \tag{A11}$$

Here we can write the signal as:

$$s_n(\tau) = \mathrm{Im}\left[ie^{-iN\varphi}\left\langle \mathrm{e}^{2\Lambda_n K}\right\rangle\right], \tag{A12}$$

where

$$\begin{aligned} e^{2\Lambda_n K} =& \mathrm{e}^{-\sum_{j=1}^{N}K_j(0)}\mathrm{e}^{2\sum_{j=1}^{N}K_j(\delta_1)}\mathrm{e}^{-2\sum_{j=1}^{N}K_j(\delta_2)}\cdots \\ & \mathrm{e}^{(-)^{n+1}2\sum_{j=1}^{N}K_j(\delta_n)}\mathrm{e}^{(-)^{n}2\sum_{j=1}^{N}K_j(\tau)}\times \\ & \mathrm{e}^{(-)^{n-1}2\sum_{j=1}^{N}K_j(\delta_n)}\cdots\mathrm{e}^{-2\sum_{j=1}^{N}K_j(\delta_2)}\times \\ & \mathrm{e}^{2\sum_{j=1}^{N}K_j(\delta_1)}\mathrm{e}^{-\sum_{j=1}^{N}K_j(0)}. \end{aligned} \tag{A13}$$

Based on the Baker-Campbell-Hausdorff (BCH) formula and $\left\langle e^A\right\rangle = e^{\langle A^2\rangle/2}$ for linear bosonic operator A [21], we get the results in main text

$$\begin{aligned} s_n(\tau) &= \mathrm{Re}\left[e^{-iN\varphi}\left\langle e^{2\Lambda_n K}\right\rangle\right] \\ &= \cos\varphi_n\exp\left(-2\chi_n\right), \end{aligned} \tag{A14}$$

with

$$\begin{aligned} \Lambda_n K &= (-)^{n+1}\sum\nolimits_{j=1}^{N}\left[(-)^n K_j(0) - K_j(\tau) + 2\sum\nolimits_{i=1}^{n}K_j(\delta_i)\right] \\ &= -\sum\nolimits_{j=1}^{N}\sum\nolimits_i\frac{\lambda_{i,j}}{2\omega_{i,j}}(b_{i,j}^\dagger y_n(\omega_i\tau) - b_{i,j}y_n^*(\omega_i\tau)), \end{aligned} \tag{A15}$$

$$y_n(z) = 1 + (-)^{n+1}e^{iz} + 2\sum_{i=1}^{n}(-)^j e^{iz\delta_j/\tau}. \quad \text{(A16)}$$

Hence, we have

$$\begin{aligned}\chi_n &= \sum_{j=1}^{N}\sum_i \frac{\lambda_{i,j}^2}{4\omega_{i,j}^2}|y_n(\omega_i\tau)|^2\left\langle b_{i,j}^\dagger b_{i,j} + b_{i,j}b_{i,j}^\dagger\right\rangle \\ &= \sum_{j=1}^{N}\int_0^{+\infty}\frac{F_n(\omega\tau)J_j(\omega)}{4\omega^2}\coth(\omega/2k_BT)\mathrm{d}\omega,\end{aligned} \quad \text{(A17)}$$

where

$$F_n(\omega\tau) = |y_n(\omega\tau)|^2, \quad \text{(A18)}$$

$$\begin{aligned}J_j(\omega) &= \sum_i |\lambda_{i,j}|^2\delta(\omega-\omega_{i,j}) \\ &= 2\alpha_j\omega\Theta(\omega_{D,j}-\omega).\end{aligned} \quad \text{(A19)}$$

When the measurement operator Σ_x is replaced with $(-i)^N\Pi_{x,N}/2$, we can transfer P-QQ metrology protocol to P-QC metrology protocol. Due to similar relation $(-i)^N\Pi_{x,N}^{ef}(\tau)/2\,|G/E\rangle = \exp\left(\pm 2\sum_{j=1}^{N}K_j(\tau)\right)|E/G\rangle$ is also held, the results of P-QC is the same as P-QQ.

Appendix B: The proof of universality for general metrology protocol

Usually in the FCE, we describe the detection of a physical field by a generator [4]

$$h_{s,c} = \sum_{j=0}^{N}\sigma_{z,j}. \quad \text{(B1)}$$

In quantum metrology, the fluctuation of $\delta\Delta_{s,c} = \delta\varphi_{s,c}/\tau$ is constrained by the generalized Heisenberg uncertainty relation

$$\delta\varphi\delta h_{s,c} \geqslant 1/(2\sqrt{l}), \quad \text{(B2)}$$

where $\langle\delta h_{s,c}\rangle^2 = \langle h_{s,c}^2\rangle - \langle h_{s,c}\rangle^2$ is the fluctuation of $h_{s,c}$ on the initial state [4]. Hence, if we express the initial state as $|\psi\rangle = \sum_{x=0}^{2^N-1}a_x|x\rangle$ and $\sum_{x=0}^{2^N-1}|a_x|^2 = 1$, we will get

$$\langle h_{s,c}\rangle = 2\sum_{x=0}^{2^N-1}c(x)\,|a|_x^2 - N, \quad \text{(B3)}$$

$$\langle h_{s,c}^2\rangle = \sum_{x=0}^{2^N-1}(2c(x)-N)^2\,|a|_x^2, \quad \text{(B4)}$$

where the function of $c(x)$ counts number of "1" (excited state) in state $|x\rangle$. The measurement uncertainty scaling as $1/N$ is equal to

$$\begin{aligned}\langle\delta h_{s,c}\rangle^2 &= \langle h_{s,c}^2\rangle - \langle h_{s,c}\rangle^2 \\ &= 2\kappa \\ &\propto N^2,\end{aligned} \quad \text{(B5)}$$

with

$$\kappa = \sum_{x,y=0}^{2^N-1}(c(x)-c(y))^2\,|a|_x^2\,|a|_y^2. \quad \text{(B6)}$$

So with the initial state $|\psi\rangle$ in the general metrology protocol, the evolution, which is denoted by R_c, can be described by Eq.(6) by dropping the noise term . The final result is:

$$\begin{aligned}p_{c,n} &= \langle\psi|\,R_c^\dagger\,|\psi\rangle\,\langle\psi|\,R_c\,|\psi\rangle \\ &= \sum_{y=0}^{2^N-1}|a_y|^2e^{ic(y)\phi}\sum_{x=0}^{2^N-1}|a_x|^2e^{-ic(x))\phi} \\ &= \sum_{x,y=0}^{2^N-1}|a_x|^2|a_y|^2e^{i(c(y)-c(x))\phi} \\ &= \sum_{x,y=0}^{2^N-1}|a_x|^2|a_y|^2\sum_{q=0}^{+\infty}\frac{[i(c(y)-c(x))\phi]^q}{q!} \\ &= \sum_{x,y=0}^{2^N-1}|a_x|^2|a_y|^2\sum_{q=0}^{+\infty}\frac{[i(c(y)-c(x))\phi]^{2q}}{(2q)!} \\ &= \sum_{x,y=0}^{2^N-1}|a_x|^2|a_y|^2\cos(c(y)-c(x))\phi,\end{aligned} \quad \text{(B7)}$$

with $\phi = \frac{4\Delta\tau}{\pi}$. So the bound of frequency uncertainty is given by

$$\begin{aligned}min\{\delta\Delta_{c,n}\} &\leqslant \left.\frac{\sqrt{p_{c,n}(1-p_{c,n})}}{|dp_{c,n}/d\Delta|\sqrt{l}}\right|_{\phi\to 2m\pi} \\ &\approx \sqrt{\frac{\pi^2}{32\tau^2l\kappa}} \\ &\propto 1/N,\end{aligned} \quad \text{(B8)}$$

where m is an integer. The above relationship shows that the general quantum metrology protocol is loyally to demonstrate any probe state with the character scaling of $1/N$ in the FCE. After taking the completely high-energy cutoff noise model into consideration, we have

$$\begin{aligned}p_n &= \sum_{x,y=0}^{2^N-1}|a_x|^2|a_y|^2e^{i(c(y)-c(x))\phi-2c(x\oplus y)\alpha\tau^6} \\ &= \sum_{x,y=0}^{2^N-1}|a_x|^2|a_y|^2\cos\left[(c(y)-c(x))\phi\right]e^{-2c(x\oplus y)\alpha\tau^6},\end{aligned} \quad \text{(B9)}$$

where $\oplus$ is a bitwise XOR operation and α is decoherence rate. Hence, we can estimate the bound of frequency uncertainty in realistic environment with DD protection

$$\begin{aligned}min\{\delta\Delta_n\} &\leqslant \left.\frac{\sqrt{p_n(1-p_n)}}{|dp_n/d\Delta|\sqrt{l}}\right|_{\substack{N\phi=2m\pi+\theta\\ \tau\approx 0.1/(\alpha N)^{1/6}\\ \theta\approx 0.1}} \\ &\approx \left.\sqrt{\frac{\theta^2\kappa/2+\xi}{l\theta^2\kappa^2|d\varphi/d\Delta|^2}}\right|_{\substack{\tau\approx 0.1/(\alpha N)^{1/6}\\ \theta\approx 0.1}},\end{aligned} \quad \text{(B10)}$$

with $\xi = 2\alpha\tau^6\sum_{x,y}^{2^N-1}c(x\oplus y)\,|a|_x^2\,|a|_y^2 \leqslant 2\alpha\tau^6N$. There-

fore, we have

$$min\{\delta\Delta_{c,n}\} \leqslant \sqrt{\frac{\theta^2\kappa/2 + 2\alpha N\tau^6}{l\theta^2\kappa^2|d\varphi/d\Delta|^2}}\Bigg|_{\substack{\tau\approx 0.1/(\alpha N)^{1/6} \\ \theta\approx 0.1}} \quad \text{(B11)}$$
$$\propto N^{-11/12}.$$

Generally, the condition $N\phi = 2m\pi + \theta$ and $\theta \approx 0.1$ is applied to Taylor expansion $\cos\theta \approx 1 - \theta^2/2$ legally. However, in the experiment with $|GHZ\rangle$ state, this condition can be replaced by $N\phi = \frac{m_1\pi}{2}$ with m_1 is an odd. For a superposition state with equal probability amplitude, the condition should be $N\phi = 2m_2\pi + \frac{m_3\pi}{2}$ with m_2 and m_3 are integers which are much smaller than N.

[1] E. M. Kessler, I. Lovchinsky, A. O. Sushkov, and M. D. Lukin, Phys. Rev. Lett. **112**, 150802 (2014).
[2] G. Arrad, Y. Vinkler, D. Aharonov, and A. Retzker, Phys. Rev. Lett. **112**, 150801 (2014).
[3] V. Giovannetti, S. Lloyd, and L. Maccone, Science **306**, 1330 (2004).
[4] V. Giovannetti, S. Lloyd, and L. Maccone, Phys. Rev. Lett. **96**, 010401 (2006).
[5] V. Giovannetti, S. Lloyd, and L. Maccone, Nat. Photon. **5**, 222 (2011).
[6] J.-M. Cui, F.-W. Sun, X.-D. Chen, Z.-J. Gong, and G.-C. Guo, Phys. Rev. Lett. **110**, 153901 (2013).
[7] C. M. Caves, Phys. Rev. D **23**, 1693 (1981).
[8] D. J. Wineland, J. J. Bollinger, W. M. Itano, F. L. Moore, and D. J. Heinzen, Phys. Rev. A **46**, R6797 (1992).
[9] F. Sun, B. Liu, Y. Gong, Y. Huang, Z. Ou, and G. Guo, EPL (Europhysics Letters) **82**, 24001 (2008).
[10] S. F. Huelga, C. Macchiavello, T. Pellizzari, A. K. Ekert, M. B. Plenio, and J. I. Cirac, Phys. Rev. Lett. **79**, 3865 (1997).
[11] R. Chaves, J. B. Brask, M. Markiewicz, J. Kołodyński, and A. Acín, Phys. Rev. Lett. **111**, 120401 (2013).
[12] L. Childress, M. V. Gurudev Dutt, J. M. Taylor, A. S. Zibrov, F. Jelezko, J. Wrachtrup, P. R. Hemmer, and M. D. Lukin, Science **314**, 281 (2006).
[13] L. T. Hall, J. H. Cole, C. D. Hill, and L. C. L. Hollenberg, Phys. Rev. Lett. **103**, 220802 (2009).
[14] M. Lovrić, H. G. Krojanski, and D. Suter, Phys. Rev. A **75**, 042305 (2007).
[15] A. Bechtold, D. Rauch, F. Li, T. Simmet, P.-L. Ardelt, A. Regler, K. Müller, N. A. Sinitsyn, and J. J. Finley, Nat. Phys. **7**, 109 (2015).
[16] A. W. Chin, S. F. Huelga, and M. B. Plenio, Phys. Rev. Lett. **109**, 233601 (2012).
[17] Y. Matsuzaki, S. C. Benjamin, and J. Fitzsimons, Phys. Rev. A **84**, 012103 (2011).
[18] T. Tanaka, P. Knott, Y. Matsuzaki, S. Dooley, H. Yamaguchi, W. J. Munro, and S. Saito, Phys. Rev. Lett. **115**, 170801 (2015).
[19] L. Cywiński, R. M. Lutchyn, C. P. Nave, and S. Das Sarma, Phys. Rev. B **77**, 174509 (2008).
[20] G. S. Uhrig, New J. Phys. **10**, 083024 (2008).
[21] G. S. Uhrig, Phys. Rev. Lett. **98**, 100504 (2007).
[22] M. Zhong, M. P. Hedges, R. L. Ahlefeldt, J. G. Bartholomew, S. E. Beavan, S. M. Wittig, J. J. Longdell, and M. J. Sellars, Nature **517**, 177 (2015).
[23] N. Bar-Gill, L. Pham, C. Belthangady, D. Le Sage, P. Cappellaro, J. Maze, M. Lukin, A. Yacoby, and R. Walsworth, Nat. Commun. **3**, 858 (2012).
[24] W. Yang and R.-B. Liu, Phys. Rev. Lett. **101**, 180403 (2008).
[25] N. Zhao, S.-W. Ho, and R.-B. Liu, Phys. Rev. B **85**, 115303 (2012).
[26] P. Sekatski, M. Skotiniotis, and W. Dür, New J. Phys. **18**, 073034 (2016).
[27] J. Zhang, A. M. Souza, F. D. Brandao, and D. Suter, Phys. Rev. Lett. **112**, 050502 (2014).
[28] J. Zhang and D. Suter, Phys. Rev. Lett. **115**, 110502 (2015).
[29] A. J. Leggett, S. Chakravarty, A. T. Dorsey, M. P. A. Fisher, A. Garg, and W. Zwerger, Rev. Mod. Phys. **59**, 1 (1987).
[30] A. M. Souza, G. A. Álvarez, and D. Suter, Phys. Rev. A **85**, 032306 (2012).
[31] L. Rondin, J.-P. Tetienne, T. Hingant, J.-F. Roch, P. Maletinsky, and V. Jacques, Rep. Prog. Phys. **77**, 056503 (2014).
[32] T. Wolf, P. Neumann, K. Nakamura, H. Sumiya, T. Ohshima, J. Isoya, and J. Wrachtrup, Phys. Rev. X **5**, 041001 (2015).
[33] F. Shi, Q. Zhang, P. Wang, H. Sun, J. Wang, X. Rong, M. Chen, C. Ju, F. Reinhard, H. Chen, et al., Science **347**, 1135 (2015).
[34] J. R. Maze, A. Drau, V. Waselowski, H. Duarte, J.-F. Roch, and V. Jacques, New J. Phys. **14**, 103041 (2012).
[35] G.-Q. Liu, X.-Y. Pan, Z.-F. Jiang, N. Zhao, and R.-B. Liu, Sci. Rep. **2** (2012).
[36] C. A. Ryan, J. S. Hodges, and D. G. Cory, Phys. Rev. Lett. **105**, 200402 (2010).
[37] L. P. Neukirch, E. von Haartman, J. M. Rosenholm, and A. N. Vamivakas, Nat. Photon. **9**, 653 (2015).
[38] M. Padgett and R. Bowman, Nat. Photon. **5**, 343 (2011).
[39] Y. Arita, M. Mazilu, and K. Dholakia, Nat. Commun. **4** (2013).